



# One-dimensional coordination polymer [Co(H<sub>2</sub>O)<sub>4</sub>(pyz)](NO<sub>3</sub>)<sub>2</sub> · 2H<sub>2</sub>O (pyz = pyrazine) with intra- and inter-chain H-bonds: structure, electronic spectral studies and magnetic properties

K. Travis Holman <sup>a</sup>, Hassan H. Hammud <sup>b,\*</sup>, Samih Isber <sup>c</sup>, Malek Tabbal <sup>c</sup>

<sup>a</sup> Department of Chemistry, Georgetown University, Washington, DC 20057-1227, USA

<sup>b</sup> Department of Chemistry, Faculty of Science, Beirut Arab University, 11-5020 Beirut, Lebanon

<sup>c</sup> Department of Physics, American University of Beirut, 11-0236 Beirut, Lebanon

Received 8 July 2004; accepted 4 November 2004

Available online 29 December 2004

## Abstract

The synthesis, structure and magnetic properties of the cobalt(II) complex (**1**) [Co(H<sub>2</sub>O)<sub>4</sub>(pyz)](NO<sub>3</sub>)<sub>2</sub> · 2H<sub>2</sub>O is reported. The compound crystallizes in the triclinic system, space group  $P\bar{1}$ , with cell constants:  $a = 7.0328(15)$  Å,  $b = 7.1255(16)$  Å,  $c = 8.4198(19)$  Å,  $\alpha = 107.226(4)^\circ$ ,  $\beta = 114.242(4)^\circ$ ,  $\gamma = 90.487(4)^\circ$ ,  $Z = 1$  and  $V = 363.35(14)$  Å<sup>3</sup>. The structure of **1** consists of elongated octahedral CoO<sub>4</sub>N<sub>2</sub> chromophores with bridging pyrazine ligands forming a one-dimensional coordination polymer along the crystallographic  $b$ -axis. The nitrate ions hydrogen-bond to the water ligands (L) and guest water (G), and form H<sub>2</sub>O(L) ··· H<sub>2</sub>O(G) ··· NO<sub>3</sub><sup>-</sup> ··· H<sub>2</sub>O(G) ··· H<sub>2</sub>O(L) chains which flank either side of the coordination polymer chains. Hydrogen-bonding is extended to neighboring chains forming a two-dimensional network. The solvent effect on the electronic spectra of pyrazine and pyrazine cobalt complex **1** has been investigated. The magnetic susceptibility of complex **1** versus temperature data showed a strong antiferromagnetic coupling between Co ions. The best fitting parameters were obtained for  $J_1/k_B = -26.4$  K,  $J_2/k_B = -2.2$  K and  $g = 2.3$ .

© 2004 Elsevier Ltd. All rights reserved.

**Keywords:** Coordination polymer; Cobalt(II) pyrazine complex; H-bond; Magnetic susceptibility

## 1. Introduction

During the last decade, there has been great interest in the design of various supramolecular self assemblies from basic building blocks. Self assembly concerns the reversible spontaneous association of a limited number of tectons under the intermolecular control of relatively labile coordination, hydrogen-bonds and dipolar interactions. The reversibility is key to the resulting systems ability to sift through the available components to form

the thermodynamically most favorable structure. The tectons come together spontaneously in a well defined way to give assemblies in one, two or three dimensions [1,2]. Molecular recognition occurring between host and guest may be an intrinsic part of the operation of the supramolecular device, which might be designed to bind and then signal the presence of a guest [3]. Supramolecular assemblies of the polymer type are of interest in the area of tunable zeolite mimics [4]. Other interests are applications in catalysis and advanced materials such as magnetic, optic and electronic materials [5–8]. In the crystal engineering ‘toolbox’ [9], hydrogen-bonding moieties are perhaps the most used implements in

\* Corresponding author. Tel.: +961 3 381862; fax: +961 1 818402.  
E-mail address: [h.hammud@bau.edu.lb](mailto:h.hammud@bau.edu.lb) (H.H. Hammud).

the design of such supramolecular systems [10], and have been particularly strongly applied towards the synthesis of molecular magnetic materials [11–16].

Because of its rod like rigidity and length, pyrazine is a good candidate for molecular building blocks. Several factors influence the specific framework structure that is formed: One factor is the role of the solvent, for example a large difference has been obtained between the double-layer structure of the solvent inclusion compound  $[\text{Ag}(\text{pyz})_2][\text{Ag}_2(\text{pyz})_5](\text{PF}_6)_3 \cdot 2\text{S}$  ( $\text{S} = \text{CH}_2\text{Cl}_2, \text{CHCl}_3, \text{CCl}_4$ ) [17] and the layer structure of the solvent-free compound  $[\text{Ag}(\text{pyz})_2](\text{PF}_6)$  [18]. The counterion can also influence the final structure, replacing the counterion  $\text{PF}_6^-$  by  $\text{SbF}_6^-$ , or  $\text{BF}_4^-$  changes the structure from the two-dimensional undulated sheet structure of  $[\text{Ag}(\text{pyz})_2](\text{PF}_6)$  [18], to the three-dimensional non-interpenetrating cubic framework of  $[\text{Ag}(\text{pyz})_3](\text{SbF}_6)$  [17], or to the interpenetrated three-dimensional structure of  $[\text{Ag}_2(\text{pyz})_3](\text{BF}_4)_2$  [19]. The specific oxidation of the metal cation can also determine the final polymer structure:  $\text{Cu}^{2+}$  is in a distorted octahedral coordination and forms a square two-dimensional network with pyrazine or substituted pyrazine [20], while  $\text{Cu}^+$  adopts a tetrahedral coordination forming three-dimensional networks with substituted pyrazine or 4,4'-bipyridine [21],  $\text{Cu}^+$  may also be trigonally coordinated by pyrazine or 4,4'-bipyridine forming three-dimensional networks or two-dimensional layers containing six-membered rings [21–26], where only  $[\text{Cu}_2(\text{pyz})_3](\text{SiF}_6)$  [22] has an interpenetrated structure. In addition the type of metal cation affects the coordination preference and thus the final polymer structure; when bonded to pyrazine,  $\text{Cu}^+$  is tetrahedral, or trigonal as just described, whereas  $\text{Ag}^+$  is found in a wide range of coordination environments: linear [19,27], trigonal [19], tetrahedral [18,19,28], square-planar, square-pyramidal and octahedral [17].

It is noted from the above discussion that the formation of coordination polymers of group IB and IIB metal ions with pyrazine has been well studied, and that more work needs to be devoted to the study of complexation with other transition metals. In the present work, we report the reaction of  $\text{Co}(\text{NO}_3)_2 \cdot 6\text{H}_2\text{O}$  with pyrazine. A new polymer compound (**1**)  $[\text{Co}(\text{pyz})(\text{H}_2\text{O})_4](\text{NO}_3)_2 \cdot 2\text{H}_2\text{O}$  is formed, which has a linear chain structure (Fig. 1). There are straight chain polymers, such as

(2)  $[\text{Co}(\text{H}_2\text{O})_4(\text{pyz})(\text{SO}_4) \cdot 2\text{H}_2\text{O}$  [29] and  $[\text{Co}(\text{acac})_2(\text{pyz})]$  (3) [30], two-dimensional sheets examples are  $[\text{CoCl}_2(\text{pyz})_2]$  [31] and  $[\text{M}(\text{pyz})_2(\text{NCS})]$  ( $\text{M} = \text{Co}, \text{Fe}$ ) [32,33], and a three-dimensional network example is  $[\text{M}(\text{pyz})(\text{Au}(\text{CN})_2)_2]$  ( $\text{M} = \text{Cu}, \text{Ni}, \text{Co}$ ) [34]. Measurement of variable temperature magnetic susceptibilities of various cobalt pyrazine complexes indicated anti-ferromagnetic behaviors [30,32–35]. The conducting properties of pyrazine metal complexes were investigated, with Fe(II) complexes showing higher conductance values compared to other metal complexes [36,37].

One important feature about the structure of compound **1** is that guest water molecules occupy void spaces in the structure and that both intra- and intermolecular hydrogen-bonding interactions are observed involving coordinated water molecules, guest water molecules and the nitrate counterions. The compound also shows weak antiferromagnetic behavior.

## 2. Experimental

All reagents were obtained from Aldrich and were used as received.

### 2.1. Synthesis of $[\text{Co}(\text{H}_2\text{O})_4(\text{pyrazine})](\text{NO}_3)_2 \cdot 2\text{H}_2\text{O}$

An acetonitrile solution (30.0 ml) of pyrazine (0.310 g, 3.87 mmol) was added to an ethanolic solution (20.0 ml) of  $\text{Co}(\text{NO}_3)_2 \cdot 6\text{H}_2\text{O}$  (0.75 g, 2.58 mmol). The mixture was refluxed for 2 h then left to stand at room temperature. Red block crystals of **1** were formed in one week. The typical yield was 92% based on  $\text{Co}(\text{NO}_3)_2 \cdot 6\text{H}_2\text{O}$ . Calc. for  $\text{C}_4\text{H}_{16}\text{CoN}_4\text{O}_{12}$ : C, 12.94; H, 4.35, N 15.10; Co, 15.88. Anal. Found: C, 12.40; H, 4.30; N, 15.30; Co, 15.80.

IR (KBr): 3319.1 (m), 3209.3 (m), 3112.9 (w), 3089.8 (w), 3051.2 (w), 1762.8 (w), 1615.2 (w), 1483.2 (m), 1433.3 (s), 1384.8 (s), 1163.0 (m), 1116.7 (m), 1055.0 (m), 987.5 (w), 825.5 (m), 788.8 (m), 474.5 (m).

### 2.2. Physical measurements

Elemental analyses of Co, C, H, N were performed by Kanti Labs Ltd., Mississauga, Canada. Infrared data

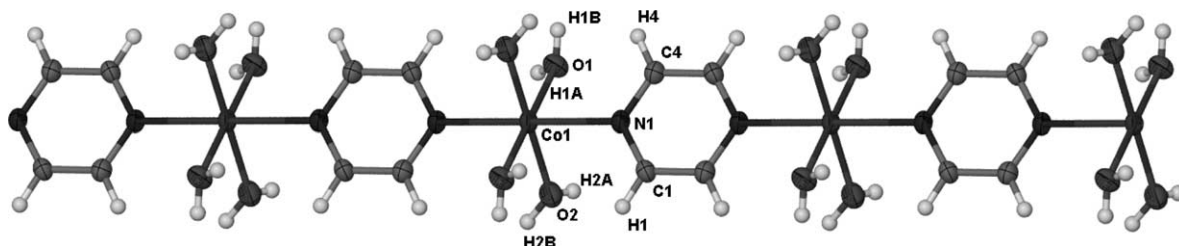


Fig. 1. Thermal ellipsoid plot of the one-dimensional polymer chain of **1**.

were collected on a Shimadzu 8300 FTIR spectrophotometer using the KBr pellet method. The electronic absorption spectra were obtained using a Ciba Corning 2800 spectrophotometer. The magnetic susceptibility of crystalline samples was measured on a Quantum Design Model 6000 Physical Property Measurement System. Diamagnetic corrections were applied using Pascal's constants.

### 2.3. Crystallography

Experimental parameters pertaining to single crystal X-ray analysis of **1** are given in Table 1. Data were collected on a single prismatic crystal measuring  $0.35 \times 0.30 \times 0.20$  mm mounted and centered on a Siemens SMART 1000 CCD platform diffractometer with graphite monochromated Mo  $K\alpha$  radiation ( $\lambda = 0.71073$  Å) at 173(2) K. The final unit cell was determined from 1222 reflections in the range of  $2.8^\circ < \theta < 28.0^\circ$ . The data were integrated using the SAINT suite of software. Lorentz and polarisation effects were accounted for using SADABS. The structure was solved by direct methods and refined iteratively via full-matrix least-squares and difference Fourier analysis using the SHELX-97 suite of software [38] and with the assistance of X-SEED [39].

The cell symmetry triclinic  $P\bar{1}$  has been preferred over monoclinic  $C2/m$  symmetry: The internal  $R$ -factor,  $R_{(\text{int})}$  for the triclinic setting is 0.036 whereas in the monoclinic setting  $R_{(\text{int})}$  it was 0.28. Structure solution and refinement in the monoclinic setting led to very high  $R$ -factors as well as unreasonable thermal parameters (and im-

posed disorder) for both pyrazine ligand and nitrate anions.

All non-hydrogen atoms were refined with anisotropic displacement parameters. The hydrogen atoms of the pyrazine ligand were placed in idealized positions and refined with a riding model whereas those on the coordinated and lattice water molecules were located and fully refined with isotropic displacement parameters. The nitrate anions are disordered and the two orientations are very well resolved, hinting at statistical disorder.

## 3. Results and discussion

### 3.1. Reaction chemistry

The title compound was obtained by the reflux reaction of hydrated cobaltous nitrate in ethanol with pyrazine in acetonitrile. Single crystals suitable for X-ray diffraction were obtained by slow evaporation of the reaction mixture after several days.

### 3.2. Description of the structure

#### 3.2.1. One-dimensional linear chain structure

The compound has a one-dimensional linear chain structure along the crystallographic  $b$ -axis, which is formed by bridging pyrazine ligands connecting the  $\text{Co}(\text{H}_2\text{O})_4$  units. A thermal ellipsoid plot of the one-dimensional polymer chain of **1** is depicted in Fig. 1. The Co atom lies at a center of symmetry and is coordinated by the oxygen atoms of four water molecules and the nitrogen atoms from two pyrazine molecules, forming an elongated octahedral cobalt coordination sphere. The oxygen atoms occupy the equatorial positions forming four short bonds with cobalt ( $\text{Co}(1)\text{--O}(1) = 2.073(2)$  Å,  $\text{Co}(1)\text{--O}(2) = 2.064(2)$  Å). The oxygens form an essentially square planar array around the central cobalt ion; the angles  $\text{O}(1)\text{--Co}(1)\text{--O}(1)$  and  $\text{O}(2)\text{--Co}(1)\text{--O}(2)$  are ideal  $180.08(7)^\circ$ , and the angles  $\text{O}(2)\text{--Co}(1)\text{--O}(1)$  are  $89.12(10)^\circ$  and  $90.88(10)^\circ$  (Fig. 1). The nitrogen atoms are located in axial positions with a perfect angle of  $180.00(7)^\circ$ . They form two long bonds with cobalt ( $\text{Co}(1)\text{--N}(1) = 2.173(2)$  Å) (Fig. 1), with values that are consistent with those found in related linear chain polymers (e.g.  $\text{Co}\text{--N} = 2.198$  Å in  $[\text{Co}(\text{H}_2\text{O})_4(\text{pyz})](\text{SO}_4) \cdot 2\text{H}_2\text{O}$  (**2**) [29] and  $2.227(2)$  Å in  $[\text{Co}(\text{acac})_2(\text{pyz})]$  (**3**) [30]). The cobalt atoms in **1** are bridged by pyrazine ligands with the nearest  $\text{Co}\cdots\text{Co}$  separation of  $7.125$  Å within the chain (Fig. 1), compared to  $7.189$  Å in **2** [29]. Each chain is surrounded by six identical chains. The separations of the metal ions between two neighboring chains are  $7.033$ ,  $8.420$  and  $8.469$  Å (see Fig. 2). This compares separations of  $6.308$ ,  $7.189$  and  $8.724$  Å in **2** [29], and  $6.290$  and  $6.27$  Å in **3** [30]. Other one-dimensional

Table 1  
Crystal data and refinement for **1**

Formula	$\text{C}_4\text{H}_{16}\text{O}_{12}\text{N}_4\text{Co}$
Color	red
$M$ ( $\text{g mol}^{-1}$ )	371.14
$T$ (K)	173(2)
Crystal system	triclinic
$\theta$ ( $^\circ$ )	2.8–28.0
Space group	$P\bar{1}$
<i>Unit cell dimensions</i>	
$a$ (Å)	7.0328(15)
$b$ (Å)	7.1255(16)
$c$ (Å)	8.4198(19)
$\alpha$ ( $^\circ$ )	107.226(4)
$\beta$ ( $^\circ$ )	114.242(4)
$\gamma$ ( $^\circ$ )	90.487(4)
$V$ (Å <sup>3</sup> )	363.35(14)
$Z$	2
$\rho_{\text{calc}}$ ( $\text{g cm}^{-3}$ )	1.696
$\mu$ ( $\text{mm}^{-1}$ )	1.248
# Unique reflections/parameters	1543/140
# Reflections $I > 2\sigma(I)$	1365
$R$ , $wR_2$ (observed data)	0.0446, 0.1133
Residual ( $\text{e} \text{ \AA}^{-3}$ )	0.801

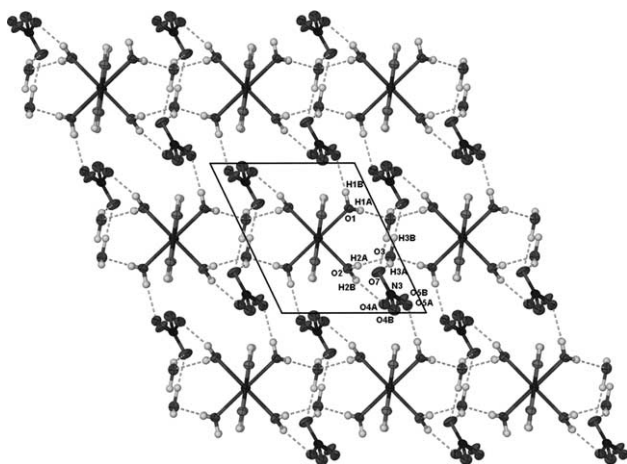


Fig. 2. Cross-sectional view in the *ac*-plane. Two-dimensional network caused by H-bonds between cobalt units in **1**.

straight chain compounds are  $[\text{Co}(\text{DBSQ})_2(\text{pyz})]$  (DBSQ = 3,6-dibutylbenzocatecholato-*O,O'*) [40] and  $[\text{Co}(\text{WO})_2(\text{pyz})]$  (WO = dimethylglyoximato) [41]. Further bridging of pyrazine ligands can lead to two-dimensional extended structures such as in  $[\text{CoCl}_2(\text{pyz})_2]$  [31] and  $[\text{Co}(\text{NCS})_2(\text{pyz})_2]$  [32]. Thus the type of anion greatly affects the final structure of the cobalt pyrazine complex: reaction of cobalt nitrate with pyrazine produces one-dimensional polymer (**1**)  $[\text{Co}(\text{pyz})(\text{H}_2\text{O})_4](\text{NO}_3)_2 \cdot 2\text{H}_2\text{O}$  with two included water molecules and no participation of nitrate in the inner coordination sphere. Notably, the reaction of cobalt nitrate with 4,4'-bipyridine, a linear *N,N'*-bidentate spacer similar to pyrazine, produces in the presence of *p*-nitroaniline (PNA) an interpenetrated square grid two-dimensional network  $[\text{Co}(\text{bipy})_2(\text{NO}_3)_2] \cdot 2\text{PNA}$  that results from a higher ligand:metal stoichiometry. In this compound, two nitrate ions occupy the axial positions within the inner coordination sphere of Co. The interpenetrated PNA forms planar networks sustained by edge-to-face interactions between the edges formed by  $\text{NO}_2$  moieties and the faces formed by the  $\text{NH}_2$  moieties [42].

### 3.2.2. H-Bond

The nitrate ions of **1** hydrogen-bond to the coordinated water ligand (L) and the lattice-included guest water (G) such that each  $[\text{Co}(\text{pyz})_2(\text{H}_2\text{O})_4]$  chain is flanked on either side by two hydrogen-bonded  $\text{H}_2\text{O}(\text{G})$  molecules and two  $\text{NO}_3^-$  ions. Thus two adjacent cobalt units within the same chain interact on each side by six extended intra-chain H-bond paths: two through  $\text{H}_2\text{O}(\text{L}) - \text{NO}_3^- - \text{H}_2\text{O}(\text{G}) - \text{H}_2\text{O}(\text{L})$ , and four through  $\text{H}_2\text{O}(\text{L}) - \text{H}_2\text{O}(\text{G}) - \text{NO}_3^- - \text{H}_2\text{O}(\text{G}) - \text{H}_2\text{O}(\text{L})$ , (Fig. 3). The bonds distances and bond angles involved in the H-bonds labelled in Fig. 3 follow. For  $\text{H}_2\text{O}(\text{L})$  with  $\text{NO}_3^-$  ions:  $\text{O}(2) \cdots \text{O}(4\text{A}) = 2.866(6)$  Å,  $\text{H}(2\text{B}) \cdots \text{O}(4\text{A}) = 2.0$  Å,  $\text{O}(2) - \text{H}(2\text{B}) \cdots \text{O}(4\text{A}) = 156^\circ$ ;

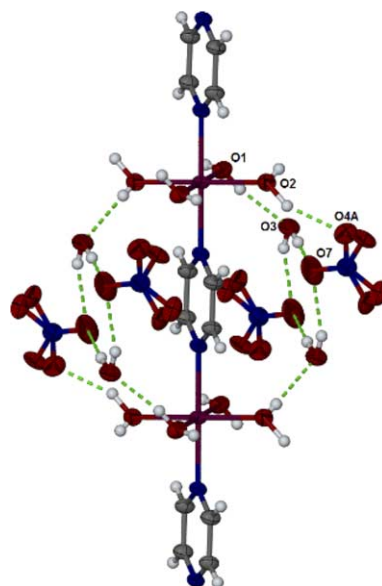


Fig. 3. Intra-chain H-bond interactions in **1**.

for  $\text{H}_2\text{O}(\text{G})$  molecules with  $\text{NO}_3^-$  ions:  $\text{O}(3) \cdots \text{O}(5\text{B}) = 2.87(1)$  Å,  $\text{H}(3\text{A}) \cdots \text{O}(5\text{B}) = 2.2$  Å,  $\text{O}(3) - \text{H}(3\text{A}) \cdots \text{O}(5\text{B}) = 149^\circ$ ,  $\text{O}(3) \cdots \text{O}(7) = 2.907(4)$  Å,  $\text{H}(3\text{A}) \cdots \text{O}(7) = 2.2$  Å,  $\text{O}(3) - \text{H}(3\text{A}) \cdots \text{O}(7) = 159^\circ$  and  $\text{O}(3) \cdots \text{O}(7) = 2.788(4)$  Å,  $\text{H}(3\text{B}) \cdots \text{O}(7) = 1.8$  Å,  $\text{O}(3) - \text{H}(3\text{B}) \cdots \text{O}(7) = 177^\circ$ ; for  $\text{H}_2\text{O}(\text{L})$  with  $\text{H}_2\text{O}(\text{G})$  molecules:  $\text{O}(1) \cdots \text{O}(3) = 2.740(3)$  Å,  $\text{H}(1\text{A}) \cdots \text{O}(3) = 2.1$  Å,  $\text{O}(1) - \text{H}(1\text{A}) \cdots \text{O}(3) = 178^\circ$  and  $\text{O}(2) \cdots \text{O}(3) = 2.704(4)$  Å,  $\text{H}(2\text{A}) \cdots \text{O}(3) = 1.9$  Å,  $\text{O}(2) - \text{H}(2\text{A}) \cdots \text{O}(3) = 170^\circ$ .

Fig. 2 shows that each linear chain is surrounded by six neighboring chains in a cross-sectional view along the *b*-axis in the *ac*-plane. Each cobalt unit interacts directly by extended inter-chain H-bonds with six neighboring units making a two-dimensional network. Complex **1** thus forms a three-dimensional supramolecular structure due to both coordination bonds (bridging by pyrazine) and H-bonds. Four types of inter-chain H-bonds paths are involved: (1)  $\text{H}_2\text{O}(\text{L}) - \text{NO}_3^- - \text{H}_2\text{O}(\text{L})$ , (2)  $\text{H}_2\text{O}(\text{L}) - \text{H}_2\text{O}(\text{G}) - \text{NO}_3^- - \text{H}_2\text{O}(\text{L})$ , (3)  $\text{H}_2\text{O}(\text{L}) - \text{H}_2\text{O}(\text{G}) - \text{H}_2\text{O}(\text{L})$ , and (4)  $\text{H}_2\text{O}(\text{L}) - \text{H}_2\text{O}(\text{G}) - \text{NO}_3^- - \text{H}_2\text{O}(\text{G}) - \text{H}_2\text{O}(\text{L})$ . The extension of intra-chain H-bonds described previously serve also in inter-chain H-bonds. The difference is in the coordinated water molecules whether they belong to the same chains or to two different chains. Thus the bonds distances and bond angles involved in inter-chain H-bonds are the same as before. Only for inter-chain H-bondings between  $\text{H}_2\text{O}(\text{L}) - \text{NO}_3^- - \text{H}_2\text{O}(\text{L})$  two additional bondings values should be listed:  $\text{O}(1) \cdots \text{O}(4\text{B}) = 2.83(1)$  Å,  $\text{H}(1\text{B}) \cdots \text{O}(4\text{B}) = 2.1$  Å,  $\text{O}(1) - \text{H}(1\text{B}) \cdots \text{O}(4\text{B}) = 149^\circ$  and  $\text{O}(1) \cdots \text{O}(5\text{A}) = 2.742(8)$  Å,  $\text{H}(1\text{B}) \cdots \text{O}(5\text{A}) = 2.0$  Å,  $\text{O}(1) - \text{H}(1\text{B}) \cdots \text{O}(5\text{A}) = 150^\circ$ .

Solvent or guest molecules are generally included in the void between chains and hydrogen-bonding interac-

tions have been also observed in related one-dimensional structures such as compound (2),  $[\text{Co}(\text{H}_2\text{O})_4(\text{pyz})](\text{SO}_4) \cdot 2\text{H}_2\text{O}$  [29],  $[\text{Co}(\text{pyz})(\text{H}_2\text{O})_4](\text{C}_8\text{H}_4\text{O}_4)$  [43] but not in  $[\text{Co}(\text{acac})_2(\text{pyz})]$  [30].

### 3.3. Discussion on IR

The absorbances between 1055.0, 1116.7 and 1163.0  $\text{cm}^{-1}$  are assignable to pyrazine bands; the peak at 474.5  $\text{cm}^{-1}$ , shifted from 417.0  $\text{cm}^{-1}$  in free pyrazine, is particularly diagnostic of bridging bidentate ligands [44–47]. Nitrate group absorbances are observed at 1615.0  $\text{cm}^{-1}$  due to an asymmetric stretch, and very strong at 1433.3 and 1384.8  $\text{cm}^{-1}$  (symmetric stretch). Broadened O–H stretches are observed for  $\text{H}_2\text{O}(\text{G})$  and  $\text{H}_2\text{O}(\text{L})$  at 3319.1  $\text{cm}^{-1}$ .

### 3.4. Discussion on electronic absorption spectra

Complex 1 shows a d–d transition at 521 nm in DMF, 536 nm in DMSO and 502 nm in pyridine.

The solvent effect on the electronic absorption spectra of pyrazine in the free state and in the complexed state in cobalt pyrazine complex 1 has been investigated, see Table 2. The absorption peak location  $Y$  ( $\lambda_{\text{max}}$  nm) of the species in a given solvent has been expressed by the following multi-parameter [48,49]:

$$Y = a_0 + a_1X_1 + a_2X_2 + a_3X_3 + a_4X_4.$$

This is amenable to solution for the intercept  $a_0$  and the coefficient  $a_i$  by multiple regression techniques. The independent variables  $X_i$  are the solvent interaction mechanisms  $E$ ,  $K$ ,  $M$  and  $N$ . The empirical solvent polarity  $E$  is sensitive to both solvent–solute hydrogen-bonding and to dipolar interactions. It is related to  $\nu$ , which is the wave number of the absorption maximum in the given solvent,  $E = 2.859 \times 10^{-3}\nu$ .

$K$  is a measure of the polarity of the solvent that depends on the solvent dielectric constant  $D$ .  $K = (D - 1)/(2D + 1)$ .

$M$  is a measure of solute permanent dipole–solvent induced dipole interactions that depend on the solvent refractive index  $n$ .  $M = (n^2 - 1)/(2n^2 + 1)$ .

$N$  is a measure of permanent dipole–permanent dipole interactions

$$N = (D - 1)/(D + 2) - (n^2 - 1)/(n^2 + 2).$$

A multiple regression analysis has been performed. In each case fits are obtained as a function of one parameter alone, two parameters or three parameters. The results are summarized in Tables 3 and 4. The  $\lambda_{\text{max}}$  studied  $\lambda_1$  and  $\lambda_2$  are for B and R bands, respectively, for pyrazine and complex 1. The values obtained are very close for both species. B bands ( $\lambda_1$ ) which originate from  $\pi$ – $\pi^*$  transitions shift to longer wavelengths in the polar solvents DMF and DMSO, while the R bands ( $\lambda_2$ ), which are due to  $n$ – $\pi^*$  transitions, shift to shorter

Table 2  
Solvent parameters and observed  $\lambda_{\text{max}}$  (nm) for cobalt pyrazine complex 1 (and pyrazine)

Solvent	$E$	$K$	$M$	$N$	$\lambda_1$	$\lambda_2$
Carbon tetrachloride	32.5	0.20	0.22	0.01	is <sup>a</sup> (266.8)	is <sup>a</sup> (313.8)
Diethyl ether	34.6	0.34	0.18	0.30	259.5 (260.0)	n <sup>c</sup> p <sup>b</sup> (315.6)
Chloroform	39.1	0.36	0.21	0.29	260.8 (261.2)	ns <sup>b</sup> (311.2)
Dimethyl formamide	43.8	0.48	0.20	0.67	271.5 (270.0)	316.2 (316.8)
Dimethyl sulfoxide	45.0	0.48	0.22	0.66	262.8 (265.0)	316.2 (317.0)
Acetonitrile	46.0	0.48	0.18	0.71	260.0 (260.5)	312.5 (313.5)
Ethanol	51.9	0.47	0.18	0.67	259.5 (259.5)	312.0 (312.5)
Methanol	55.5	0.48	0.17	0.71	261.2 (260.0)	310.0 (310.0)
Water	63.1	0.49	0.17	0.76	260.0 (260.6)	300.0 (301.0)

<sup>a</sup> Complex 1 is insoluble.

<sup>b</sup> No characteristic peak observed.

Table 3  
Regression analysis for cobalt pyrazine complex 1 (and pyrazine) using  $E$ ,  $K$ ,  $M$ ,  $N$  at  $\lambda_1$

Parameters	$a_0$	$a_1$	$a_2$	$a_3$	$a_4$	MCC
$E$	265.189 (269.238)	−0.069 (−0.145)				0.157 (0.383)
$K$	253.636 (265.874)	18.495 (−7.743)				0.279 (0.208)
$M$	245.210 (238.932)	88.492 (123.245)				0.414 (0.676)
$N$	259.449 (264.195)	4.131 (−2.961)				0.194 (0.209)
$EK$	252.586 (268.726)	−0.361 (−0.212)	59.035 (8.580)			0.614 (0.409)
$EM$	241.16 (234.544)	0.042 (0.041)	99.461 (136.301)			0.422 (0.681)
$KM$	231.787 (232.900)	24.158 (6.736)	102.332 (139.906)			0.548 (0.693)
$EKM$	242.919 (234.172)	−0.273 (−0.024)	51.726 (8.132)	46.473 (135.856)		0.636 (0.694)
$EKMN$	196.234 (253.723)	−0.298 (−0.196)	362.369 (−516.78)	−110.923 (−547.90)	−102.996 (532.256)	0.691 (0.902)

Table 4

Regression analysis for cobalt pyrazine complex **1** (and pyrazine) using  $E$ ,  $K$ ,  $M$ ,  $N$  at  $\lambda_2$ 

Parameters	$a_0$	$a_1$	$a_2$	$a_3$	$a_4$	MCC
$E$	349.778 (328.657)	-0.759 (-0.356)				0.949 (0.720)
$K$	599.150 (316.688)	-600.000 (-10.262)				0.634 (0.210)
$M$	270.019 (287.605)	220.345 (128.874)				0.724 (0.540)
$N$	413.306 (315.062)	-146.636 (-5.055)				0.925 (0.272)
$EK$	453.342 (326.066)	-0.669 (-0.698)	-225.304 (43.418)			0.972 (0.912)
$EM$	345.843 (321.599)	-0.732 (-0.318)	13.772 (27.727)			0.950 (0.726)
$KM$	516.233 (283.904)	-502.832 (4.134)	194.336 (139.099)			0.894 (0.545)
$EKM$	456.477 (319.617)	-0.558 (-0.663)	-262.775 (43.335)	49.314 (25.355)		0.978 (0.915)
$EKMN$	321.726 (336.260)	-0.488 (-0.785)	295.952 (-31.273)	-118.938 (39.824)	-151.569 (32.954)	0.992 (0.941)

wavelengths in hydrogen-bonding solvents. The data for  $\lambda_1$  shows good dependence of the shift in  $\lambda_{\max}$  on  $M$ , the data indicates improvement in the fit in going from one parameter to two, three and four parameter correlations. The data for  $\lambda_2$  shows very good dependence of the shift in  $\lambda_{\max}$  on  $E$ ,  $K$ ,  $M$  and  $N$  parameters. The multiple correlation coefficients MCC in the complex are higher than in the free pyrazine.

### 3.5. Magnetic study

The temperature dependence of the inverse magnetic susceptibility for compound **1** as a function of the temperature in the range 2–300 K is shown in Fig. 4 ( $\chi_M^{-1}$  versus  $T$ ). This figure shows that  $\chi_M^{-1}$  follows the Curie–Weiss law, and decreases linearly as the temperature decreases down to 25 K. The best fitting to a straight line yields a negative Curie–Weiss temperature of -16.8 K, indicative of a strong antiferromagnetic coupling between Co ions. At 300 K  $\chi_M T$  versus  $T$  is equal to 2.985 cm<sup>3</sup> K mol<sup>-1</sup> which is quite different from the value of 2.1 cm<sup>3</sup> K mol<sup>-1</sup> reported by Ma et al. [30].

The  $\chi_M T$  versus  $T$  curve exhibits a continuous decrease from 300 to 2 K as the temperature is lowered. Such behavior is characteristic for Co(II) complexes,

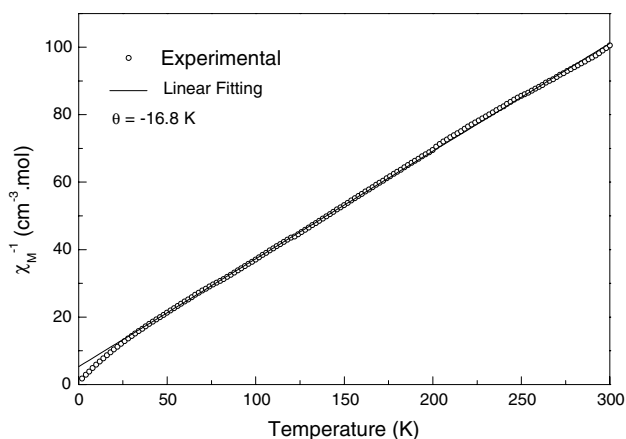


Fig. 4. Inverse of the molar magnetic susceptibility of **1** vs. temperature, the straight line represents the best fit to a Curie–Weiss law obtained for  $\theta = -16.8$  K.

due to single ion anisotropy with some contribution of antiferromagnetic exchange between the Co(II) centers. The magnetic coupling can be mediated through extensive intra-chain as well as inter-chain H-bondings interactions between the cobalt atoms. The experimental susceptibility data has been tentatively fitted for  $S = 3/2$  using the classical spin model for the magnetic susceptibility of an infinite chain derived by Fisher [50]. Thus, the best fitting gave the following values for the parameters:  $J = -1.1$  cm<sup>-1</sup>,  $g = 2.55$ . However, the experimental data did not match the calculated ones especially at low temperature, and the Landé factor obtained does not reflect the ground of Co as seen in many systems [51–55]. A three-dimensional magnetic behavior with two exchange couplings rather than one should be considered. Also the analysis of magnetic data for cobalt complexes is complicated by single ions effects such as spin–orbit coupling, distortion from regular stereochemistry, electron delocalization, crystal field mixing of excited states into the ground state and by magnetic exchange interactions [56]. To improve the correlation between the experimental and theoretical data we attempted to include a second exchange coupling constant, thus our model consists of two linear chains corresponding to the shortest Co distances deduced from the X-rays data that are 7.125, 7.033, 8.420 and 8.469 Å. We calculated the spin Hamiltonian and the magnetic susceptibility of the linear chains taking into account two isotropic exchange-coupling constants,  $J_1$  and  $J_2$  [57]. For simplicity reasons each linear chain is considered to be a closed triplet that contains three Co ions interacting among themselves [58]. Thus, the spin Hamiltonian of a closed triplet is given by

$$H = -2J_i(S_1S_2 + S_1S_3 + S_2S_3) \quad i = 1, 2. \quad (1)$$

The magnetic susceptibility was calculated using the expression given by Spasojevic et al. [59]

$$\chi = \left( \frac{g\mu_B}{k_B T} \right)^2 \left( \frac{\sum_{S,m} m^2 \text{Exp}(E(\alpha, S, m)/k_B T)}{\sum_{S,m} \text{Exp}(E(\alpha, S, m)/k_B T)} - \left( \frac{\sum_{S,m} m \text{Exp}(E(\alpha, S, m)/k_B T)}{\sum_{S,m} \text{Exp}(E(\alpha, S, m)/k_B T)} \right)^2 \right), \quad (2)$$

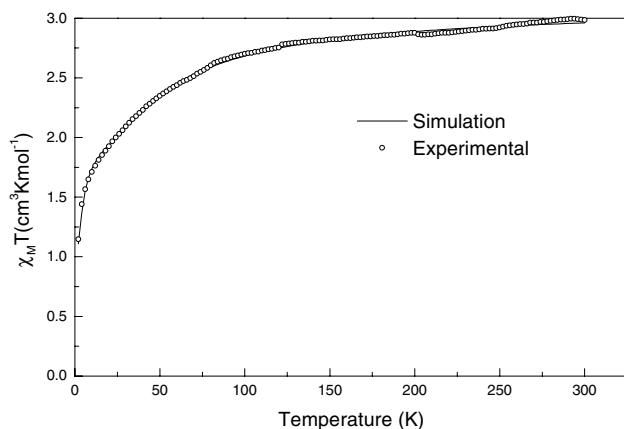


Fig. 5.  $\chi_M T$  vs. temperature for **1**, the continuous line represents the best fitting using Eq. (2).

where  $\mu_B$  is the Bohr magneton  $k_B$  is the Boltzman constant,  $g$  is the Landé factor and  $\alpha$  is a notation for all quantum numbers besides  $S$  and  $m$ . Using this model the fit has been improved tremendously, as shown in Fig. 5. The best fitting parameters were obtained for  $J_1/k_B = -26.4$  K,  $J_2/k_B = -2.2$  K and  $g = 2.3$ .

#### Appendix A. Supplementary data

CCDC No. 211146 contains the supplementary crystallographic data for this paper. These data can be obtained free of charge at [www.ccdc.cam.ac.uk/conts/retrieving.html](http://www.ccdc.cam.ac.uk/conts/retrieving.html), or from the Cambridge Crystallographic Data Centre (CCDC), 12 Union Road, Cambridge CB2 1EZ, UK (fax: +44 1223 336033; e-mail: [deposit@ccdc.cam.ac.uk](mailto:deposit@ccdc.cam.ac.uk)). Supplementary data associated with this article can be found, in the online version, at [doi:10.1016/j.poly.2004.11.017](https://doi.org/10.1016/j.poly.2004.11.017).

#### References

- [1] J.S. Lindsey, *New J. Chem.* 15 (1991) 153.
- [2] D. Braga, F. Grepioni, G.R. Desiraju, *Chem. Rev.* 98 (1998) 1375.
- [3] J.-M. Lehn, *Supramolecular Chemistry: Concept and Perspectives*, VCH, Weinheim, 1995, p. 89.
- [4] C.J. Jones, *Chem. Soc. Rev.* 27 (1998) 289.
- [5] B.F. Abrahams, B.F. Hoskins, D.M. Michael, R. Robson, *Nature* 369 (1994) 727.
- [6] S. Kitagawa, M. Kondo, *Bull. Chem. Soc. Jpn.* 71 (1998) 1.
- [7] O.M. Yaghi, G. Li, H. Li, *Nature* 378 (1995) 703.
- [8] S.S.Y. Chui, S.M.F. Lo, J.P.H. Charmant, A.G. Orpen, I.D. Williams, *Science* 283 (1999) 1148.
- [9] D. Braga, F. Grepioni, G.R. Desiraju, *Chem. Rev.* 98 (1998) 1375.
- [10] M.J. Zaworotko, *Chem. Soc. Rev.* (1994) 283.
- [11] C.J. O'Connor, E. Sinn, *Inorg. Chem.* 20 (1981) 545.
- [12] A. Lang, Y. Pei, L. Ouahab, O. Khan, *Adv. Mater.* 8 (1996) 60.
- [13] J. Veciana, J. Cirujeda, C. Rovira, E. Molins, J.J. Novoa, *J. Phys. Chem.* 100 (1996) 1667.
- [14] N. Yoshioka, M. Irisawa, Y. Mochizuki, T. Kato, H. Inoue, S. Ohba, *Chem. Lett.* (1997) 251.
- [15] O. Kahn (Ed.), *Magnetism: A Supramolecular Function*, Kluwer, Dordrecht, 1996.
- [16] M.M. Matsushita, A. Izuoka, T. Sugawara, T. Kobayashi, N. Wada, N. Takeda, M. Ishikawa, *J. Am. Chem. Soc.* 119 (1997) 4369.
- [17] L. Carlucci, G. Cianni, D.M. Proserpio, A. Sironi, *Angew. Chem., Int. Ed. Engl.* 34 (1995) 1895.
- [18] L. Carlucci, G. Cianni, D.M. Proserpio, A. Sironi, *Inorg. Chem.* 34 (1995) 5698.
- [19] L. Carlucci, G. Cianni, D.M. Proserpio, A. Sironi, *J. Am. Chem. Soc.* 117 (1995) 4562.
- [20] T. Otieno, S.J. Rettig, R.C. Thompson, J. Trotter, *Inorg. Chem.* 32 (1993) 4384.
- [21] P. Halasyamani, K.R. Heier, M.J. Willis, C.L. Stern, K.R. Poppelmeier, *Z. Anorg. Allg. Chem.* 622 (1996) 479.
- [22] L.R. MacGillivray, S. Subramanian, M.J.J. Zaworotko, *J. Chem. Soc., Chem. Commun.* (1994) 1325.
- [23] T. Otieno, S.J. Rettig, R.C. Thompson, J. Trotter, *Inorg. Chem.* 32 (1993) 1607.
- [24] S. Kitagawa, M. Munakata, T. Tanimura, *Inorg. Chem.* 31 (1992) 31.
- [25] S. Kitagawa, S. Katawa, M. Kondo, Y. Nozaka, M. Munakata, *Bull. Chem. Soc. Jpn.* 66 (1993) 3387.
- [26] M.M. Turnbull, G. Pon, R.D. Willett, *Polyhedron* 10 (1991) 1835.
- [27] O.M. Yaghi, H. Li, *J. Am. Chem. Soc.* 118 (1996) 295.
- [28] L. Carlucci, G. Ciani, D.M. Proserpio, A. Sironi, *J. Chem. Soc., Chem. Commun.* (1994) 2755.
- [29] Th. Fetzter, R. Jooss, A. Lentz, T. Debaerdemaeker, *Z. Anorg. Allg. Chem.* 620 (1994) 1750.
- [30] B.-Q. Ma, S. Gao, T. Yi, G.-X. Xu, *Polyhedron* 20 (2001) 1255.
- [31] P.W. Carreck, M. Goldstein, E.M. McPartlin, W.D. Unsworth, *J. Chem. Soc., Dalton Trans.* (1971) 1634.
- [32] J. Lu, T. Paliwala, S.C. Lim, C. Yu, T. Niu, A.J. Jacobson, *Inorg. Chem.* 36 (1997) 923.
- [33] J.A. Real, G.D. Munno, M.C. Munoz, M. Julve, *Inorg. Chem.* 30 (1991) 2701.
- [34] D.B. Leznoff, B.-Y. Xue, C.L. Stevens, A. Storr, R.C. Thompson, B.O. Patrick, *Polyhedron* 20 (2001) 1247.
- [35] R.L. Carlin, D.W. Carnegie, J. Bartolome, D. Gonzalez, L.M. Floria, *Phys. Rev. B: Condens. Matter* 32 (11) (1985) 7476.
- [36] J. Straehle, F. Kubel, W. Hiller, R. Dantona, *Mol. Cryst. Liq. Cryst.* 81 (1–4) (1982) 265.
- [37] M. Hanak, W. Kobel, J. Metz, M. Mezger, G. Pawlowski, O. Schneider, H.J. Schulze, L.R. Subramanian, *Mater. Sci.* 7 (2–3) (1981) 185.
- [38] G.M. Sheldrick, *SHELX-97*, University of Göttingen, Germany, 1997.
- [39] L.J. Barbour, *J. Supramol. Chem.* 1 (2001) 189. <http://x-seed.net/>.
- [40] O.-S. Jung, C.G. Pierpont, *J. Am. Chem. Soc.* 116 (1994) 2229.
- [41] F. Kubel, J. Strahle, *Z. Naturforsch., Teil B* 36 (1981) 441.
- [42] B. Moulton, E.B. Rather, M.J. Zaworotko, *Cryst. Eng.* 4 (2001) 309.
- [43] S.-Y. Yang, L.-S. Long, R.-B. Huang, L.-S. Zheng, S.W. Ng, *Acta Crystallogr., Sect. E* 59 (2003) m961.
- [44] J.S. Haynes, J.R. Sams, R.C. Thompson, *Inorg. Chem.* 25 (1986) 3740.
- [45] J.S. Haynes, J.R. Sams, R.C. Thompson, *Can. J. Chem.* 66 (1988) 2079.
- [46] T. Otieno, S.J. Rettig, R.C. Thompson, J. Trotter, *Can. J. Chem.* 67 (1989) 1964.
- [47] T. Otieno, S.J. Rettig, R.C. Thompson, J. Trotter, *Can. J. Chem.* 68 (1990) 1901.
- [48] M.S. Masoud, H.H. Hammud, *Ultra Science* 12-1 (2000) 12.
- [49] M.S. Masoud, H.H. Hammud, *Spectrochim. Acta A* 57 (2001) 977.
- [50] M.E. Fisher, *Am. J. Phys.* 32 (1964) 343.

- [51] A. Abragam, B. Bleaney, *Electron Paramagnetic Resonance of Transition Ions*, Clarendon Press, Oxford, 1970.
- [52] S. Isber, M. Averous, Y. Shapira, V. Bindilatti, A.N. Anisimov, N.F. Olivera, V.M. Orera, M. Demianiuk, *Phys. Rev. B* 51 (1995) 15211.
- [53] V. Bindilatti, Y. Shapira, M. Goiran, F. Yang, S. Isber, M. Averous, M. Demianiuk, *Phys. Rev. B* 50 (1994) 14464.
- [54] I.M. Villeret, S. Rodriguez, E. Kartheuser, *Phys. Rev. B* 41 (1990) 10028.
- [55] A. Lewicki, A.I. Schindler, I. Miotkowski, B.C. Grooker, J.K. Furdyna, *Phys. Rev. B* 43 (1991) 5713.
- [56] S. Emori, M. Inoue, M. Kubo, *Coord. Chem. Rev.* 21 (1976) 1.
- [57] T. Christidis, S. Isber, M. Tabbal, U. Kortz, D. Ravot, *J. Magn. Mater.* 242 (2002) 939.
- [58] S. Isber, P. Masri, S. Charar, X. Gratens, S.K. Misra, *J. Phys. C* 9 (1997) 10023.
- [59] V. Spasojevic, A. Bojorek, A. Szytula, W. Giritat, D. Mitic, *Phys. Stat. Sol. B* 165 (1991) 555.